Article

MS/MS-guided isolation of clarinoside, a new anti-inflammatory pentalogin derivative

Coralie Audoin [1], Adam Zampalégré [1], Natacha Blanchet [1], Alexandre Giuliani [2,3], Emmanuel Roulland [4], Olivier Laprévote [4,5] and Grégory Genta-Jouve [4,*]

[1]   Laboratoires Clarins, 5 rue Ampère, 95300 Pontoise, France;
[2]   DISCO Beamline, Synchrotron SOLEIL, 91192, Gif-sur-Yvette, France ;
[3]   UAR1008, CEPIA, INRA, 44316 Nantes, France ;
[4]   C-TAC, UMR 8638 CNRS, Université Paris Descartes, Sorbonne Paris Cité, Faculté de Pharmacie de Paris, 4 avenue de l'Observatoire, 75006 Paris, France;
[5]   Department of Biochemistry, Hôpital Européen Georges Pompidou, AH-HP, 75015 Paris, France
*   Correspondence: gregory.genta-jouve@parisdescartes.fr; Tel.: +33 173 531 585

Abstract: Re-investigation of the chemical composition of the annual plant *Mitracarpus scaber* Zucc. led to the identification of clarinoside, a new pentalogin derivative containing a rare quinovose moiety, and the known compound harounoside. While the planar structure was fully determined using tandem MS and quantum mechanics calculations (QM), the tridimensional structure was unravelled after isolation and NMR analysis. The absolute configuration was assigned by comparison of experimental and theoretical SRCD spectra. Both compounds were tested for anti-inflammatory activity and compound **1** showed the ability to inhibit the production of interleukin-8 (Il-8) with an IC_{50} of 9.17 μM

Keywords: *Mitracarpus scaber* Zucc. ; pentalogin ; anti-inflammatory ; MS/MS ; Il-8 ;

1. Introduction

Mass spectrometry has become a very convenient technique for the targeted search of new bioactive metabolites[1,2] and the recent introduction of the Global Natural Product Social molecular networking (GNPS) Web-platform (http://gnps.ucsd.edu) has enabled the quick and automatic spectral mining of MS/MS spectra [3]. In our ongoing research for bioactive compounds, we decided to re-investigate the chemical composition of *Mitracarpus scaber* Zucc. using a MS/MS-guided approach. *M. scaber* is an annual plant used in African traditional medicine endowed with antifungal, antimicrobial and anti-inflammatory properties [4,5]. Indeed, in West Africa, the leaves of *M. scaber* are widely used for headache, toothache, amenorrhea, dyspepsia, hepatic diseases, venereal diseases, leprosy and for the treatment of skin diseases such as scabies, infectious dermatitis and eczema. It is well known to contain phenols[5], flavonoid glycosides[5], furanocoumarines[5], terpenes[6], alkaloids[7] and pentalongin derivatives[8,9]. Herein, we report the identification of clarinoside (**1**), a new pentalongin derivative exhibiting the rare quinovose moiety along with the known harounoside (**2**). Both compounds were tested for anti-inflammatory activity by evaluating their ability to inhibit the production of interleukin-8 (Il-8).
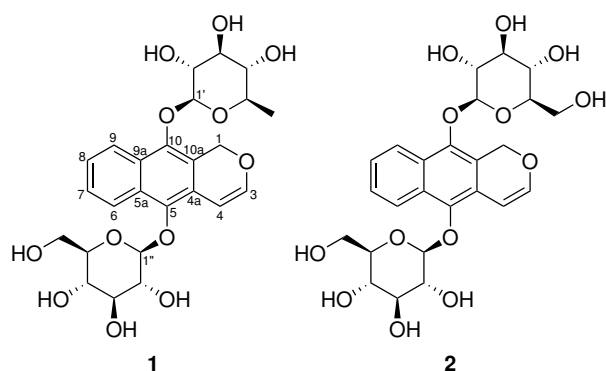
Figure 1. Structure of clarinoside (**1**) and harounoside (**2**)

2. Results

The analysis started by the creation of a molecular network of the ethanolic extract of *M. scaber*. The data-dependent analysis (DDA) LC-MS/MS data were uploaded to the GNPS platform and a network was generated using the parameters listed in the materials and method section below (Figure 2). As an anchor (reference) compound, harounoside (**2**) was used. Its node was quickly "illuminated" using the high resolution MS data and fragmentation pattern. The *m/z* value at 561.159 corresponding to the [M+Na]$^+$ adduct of **2** was identified and two diagnostic MS/MS fragments were present on the spectrum (see supporting information): a first one resulting from the cleavage of the glycosidic bond between the aglycone and a glucose moiety at *m/z* 399.1080 [M-Glc+Na]$^+$ and a second one at *m/z* 236.0452 resulting from the cleavage of the second O–C between the aglycone and the other glucose [M-2Glc+Na]$^{•+}$. In order to seek the structurally related compounds, the cluster was further studied by annotating the edges with *m/z* differences corresponding to known (bio)chemical modifications implemented in the MetaNetter 2 package [10]. Out of the 307 nodes of the network, one node directly connected to harounoside (**2**) with a *m/z* difference of -15.995 attracted our attention. According to the biotransformation list available in the MetaNetter package, this difference corresponded to a dehydroxylation.
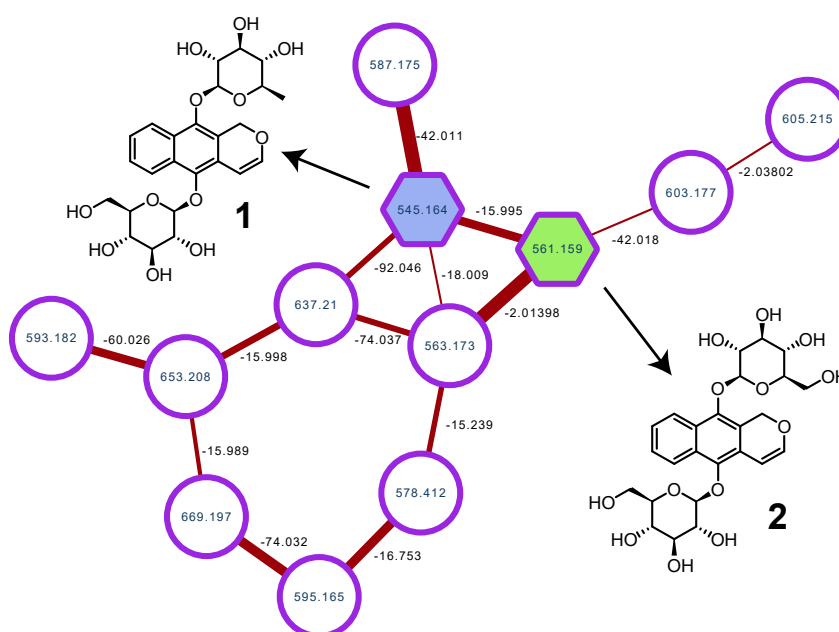

Figure 2. Selected cluster containing clarinoside (**1**) and harounoside (**2**)

Considering the structure of **2**, the dehydroxylation could occur at several positions of each of the two sugars; in order to know on which side of the compound **2** the dehydroxylation site was located, the fragmentation of both glucose moieties was studied using quantum mechanics (QM). After examination of the MS/MS spectrum, the sequential losses of two glucoses were observed. The nature of the sugar being the same at C-5 and C-10, the energy level of the two O–C bonds was only related to the position on the aglycone. In order to confirm that hypothesis, the energy profile of the homolytic dissociation was predicted using the B3LYP method at the STO-3G level (See supporting information). The calculations predicted a difference of ca. +2.5 eV in favor of the O–C1", indicating that the first fragment observed at m/z 399.1080 was related to the loss of one glucose at C-10. This energy difference was very supportive; based on these theoretical results, an energy resolved mass spectrometry (ERMS) study [11] was undertaken in order to determine the stability of the two O–C bonds (O–C1" and O–C1') of compound **2**. After selection of the parent ion at m/z 561.16, the intensity of the ion at m/z 399.11 was recorded using an increasing value of collision energy (CID). After the complete extinction of the parent ion (figure 3A), the daughter ion at m/z 399.11 was then fragmented into one major ion at m/z 185.04 using the same approach (figure 3B). As shown in Figure 3, the O–C1' bond linking the aglycone to the glucose moiety is weaker than the O–C1" as it requires a lower CE value for a 50% dissociation (ca. 15 and 17 for O–C1' and O–C1" respectively).
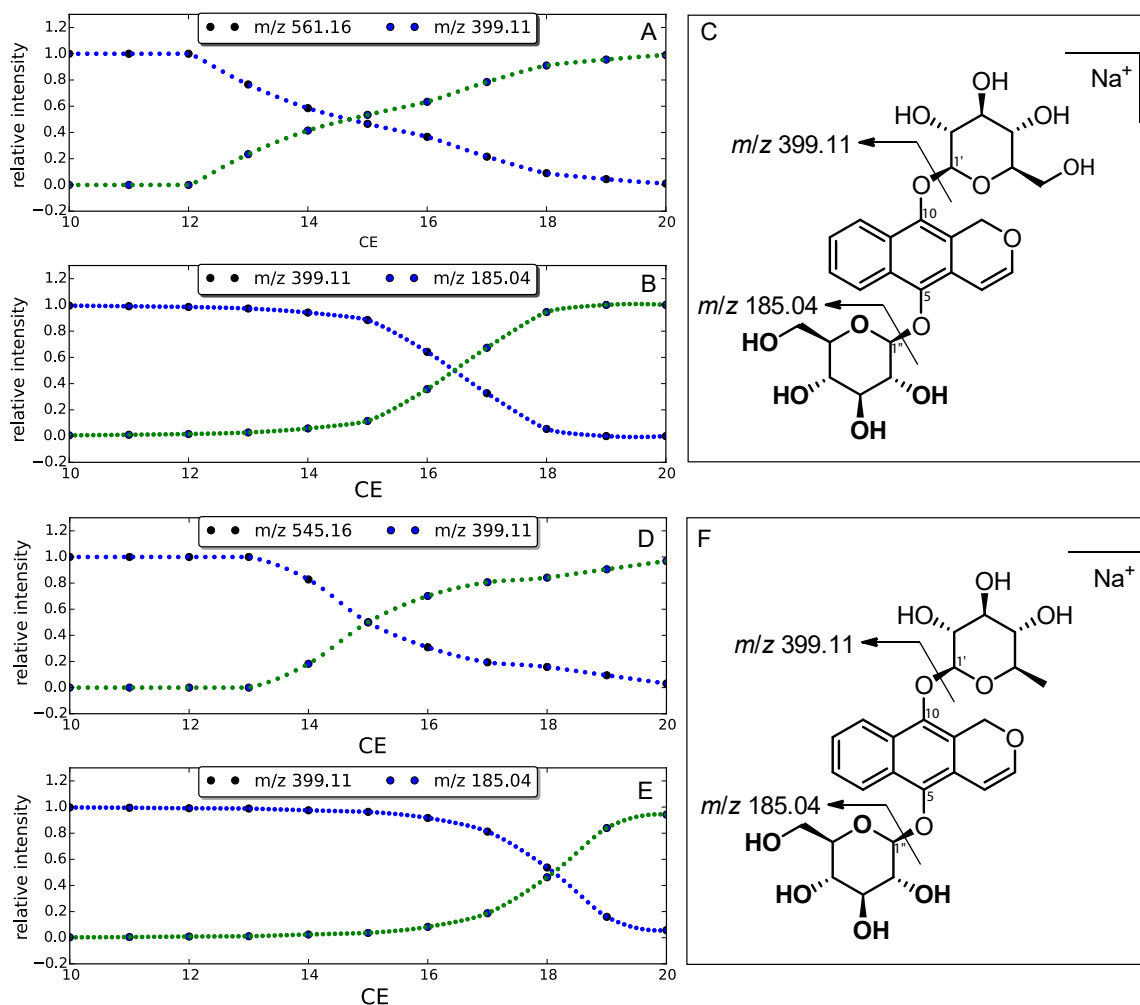

Figure 3. Plot of relative ion current versus collision energy corresponding to m/z 561.16 vs 399.10 (**A**) and m/z 399.10 vs 185.04 (**B**); **C**: MS/MS Fragments of **2**. Plot of relative ion current versus collision energy corresponding to m/z 545.16 vs 399.10 (**D**) and m/z 399.10 vs 185.04 (**E**); **F**: MS/MS Fragments of **1**.

The experimental data confirmed the QM predicted values and the same ERMS approach was used for compound **1**. As observed on figures 3D and 3E, an increase of the CE value was required in order to produce the ion at m/z 185.05 (ca. 15 and 18 for O–C1' and O–C1" respectively). Those results clearly confirmed the position of the deoxyhexose moiety at C-10. The planar structure was further confirmed by the identification of the neutral loss of 146.0605 Da resulting from the difference between the [M+Na]$^+$ ion at m/z 545.1685 and the fragment at m/z 399.1080. In parallel with the loss of 162.05 Da corresponding to a glucose moiety (observed for **2**), the loss of 146.0605 was consistent with a deoxyhexose such as fucose, rhamnose or quinovose. Unfortunately, and despite the use of a recent methodology to distinguish the mono-saccharides using MS/MS[12], it was not possible to determine the relative stereo-chemistry of the sugar moieties using MS analysis only, so the isolation of compound **1** was undertaken.

After a reverse phase HPLC purification, 84 mg of compound **1** was obtained and a full set of NMR experiments was performed. The structure of the aglycone was confirmed by comparison of the ^{1}H and ^{13}C NMR chemical shifts (see table 1). The nature of the sugar was determined by taking advantage of the newly published methodology by Giner *et al.*[13] which is based on an acid-promoted hydrolysis of the studied compound performed directly in the deuterated NMR solvent. Looking at the ^{1}H NMR spectrum, the doublets at δ 4.66 (J = 7.7 Hz) and 4.79 (J = 7.8 Hz) ppm clearly confirmed a glucose and a quinovose moiety (see supporting information). According to the ERMS data, the quinovose was located at C-10 and this was confirmed by the two ^3J coupling between H-1'/C-10 and H-1"/C-5 on the HMBC spectrum. The detailed NMR data are given in the table 1.

Table 1. ^{1}H and ^{13}C NMR data for **1** at 600 MHz in CD$_3$OD (δ_H in ppm)

	clarinoside (**1**)					harounoside (**2**) ref [8]		
no.	δ_H (multiplicity, J)	δ_C	no.	δ_H (multiplicity, J)	δ_C	no.	δ_H	δ_C
1	5.29 (dd, 40.7, 13.8 Hz)	65.2	1'	4.66 (d, 7.8)	106.2	1	5.39; 5.30	65.4
3	6.67 (dd, 14.4, 5.9 Hz)	147.8	2'	3.61 (dd, 9.0, 7.8)	75.9	3	6.68	147.8
4	6.66 (dd 14.4, 5.9 Hz)	102.1	3'	3.38 (t, 9.0)	77.7	4	6.64	102.2
4a		121.6	4'	3.11 (t, 9.0)	73.5	4a		121.7
5		143.3	5'	3.11 (m)	77.8	5		143.4
5a		131.0	6'	1.21 (d, 5.4)	18.1	5a		131.0
6	8.43 (d, 8.2 Hz)	124.7	1"	4.79 (d, 7.8)	106.9	6	8.42	124.7
7	7.44 (dt, 8.2, 1 Hz)	127.0	2"	3.65 (m)	75.8	7	7.43	127.0
8	7.40 (dt, 8.2, 1 Hz)	126.2	3"	3.46 (m)	71.5	8	7.39	126.3
9	8.41 (d, 8.2 Hz)	123.7	4"	3.14 (m)	76.9	9	8.43	123.7
9a		129.1	5"	3.47 (t, 9.0)	78.0	9a		129.1
10		144.9	6"	3.67 (m)	62.7	10		145.0
10a		122.6				10a		122.7

The absolute configuration of compound **1** was determined by comparison of a synchrotron radiation circular dichroism (SRCD) spectrum with a theoretical electronic circular dichroism (ECD) spectrum (Figure 4). Unexpectedly, the ECD spectrum was quite complex with four Cotton effects (CE) of alternative signs. The calculations were run on the four diasteroisomers, i.e., *D*-Glc/*D*-Qui, *D*-Glc/*L*-Qui, *L*-Glc/*D*-Qui and *L*-Glc/*L*-Qui. While the absolute *D* configuration of the glucose moiety was expected, as it is well known that higher plants produce only this enantiomer [14], the absolute configuration of the quinovose moiety was not obvious because the quinovose can originate from either *D*-glucose [15] or *L*-fucose [16].

A very good agreement was observed between the *D*-Glc/*D*-Qui theoretical and the experimental spectra (figure 4). The compound **1** could be named 5,10-dihydroxy-2*H*-naphtho[2,3-b]-pyran-5-*β*-*D*-glucopyranosyl-10-*β*-*D*-quinovopyranoside.
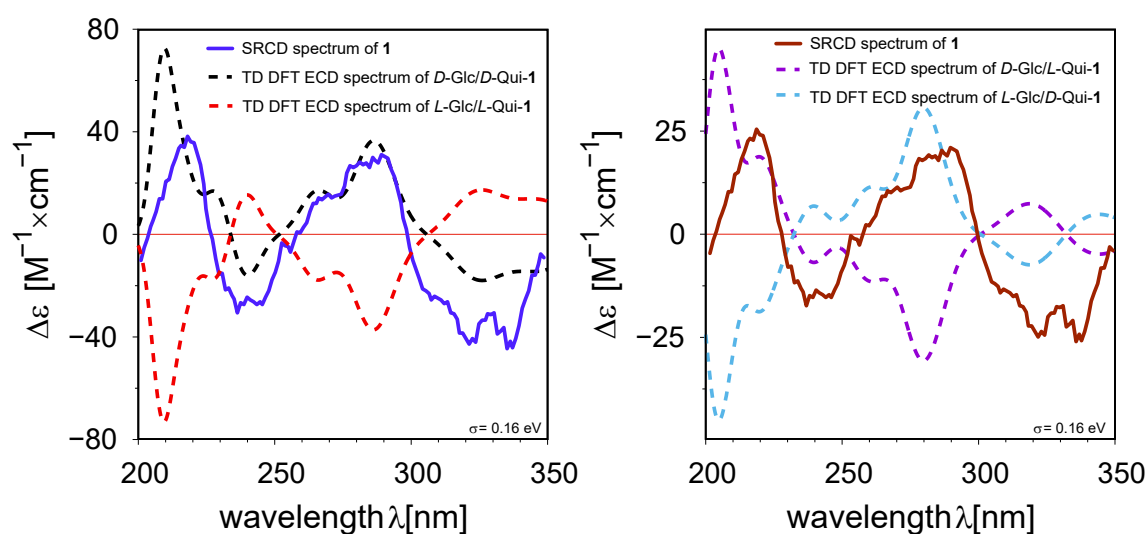
Figure 4. Overlay of SRCD and TD DFT spectra of **1**

Both compounds **1** and **2** were tested for anti-inflammatory activity by measuring their ability to inhibit the production of interleukin-8 (Il-8), one of the key mediators associated with inflammation[17,18]. After exposure to the tumor necrosis factor alpha (TNFα) at 0.5 ng mL^{-1} for 24 hours, the production of Il-8 was measured and compared to the known anti-inflammatory standard epigallocatechin gallate (EGCG). As shown in Figure 5, the TNFα is inducing the production of Il-8 of 398.37$\pm$24.09 pg/mg of total protein while the addition of EGCG at 21.8 μM allows a return to the basal threshold of 33.01$\pm$2.12 pg/mg of total protein. Although the two compounds were tested
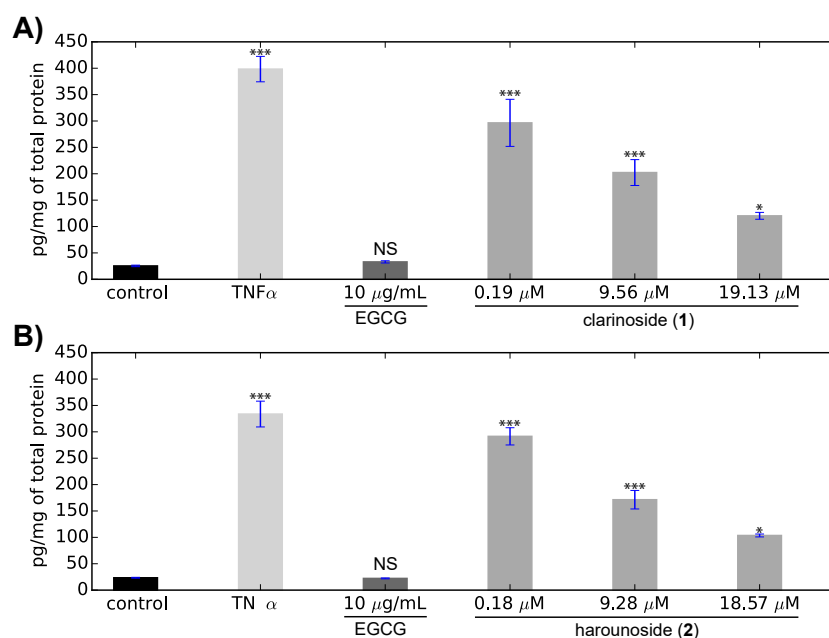

Figure 5. Inhibition of the interleukin-8 (Il-8) production: **A** clarinoside (**1**); **B** harounoside **(2)**; Means $\pm$ SD are shown. NS. not significant; *$P < 0.05$; ***$P < 0.001$

during two independent tests, the differences in the measured concentrations (i.e., the production of Il-8 and its inhibition) were observed in both experiments. A good correlation (R^2=0.996) is observed between the inhibition of the production of Il-8 and the concentration of clarinoside (**1**). A IC$_{50}$ of 9.17

100 μM was measured while a total inhibition of the Il-8 production at 36 μM can be extrapolated. The
101 IC$_{50}$ of **1** is of the same order of magnitude as that of EGCG (10.9 μM[19]), although slightly lower.
102 Interestingly, the IC$_{50}$ of **2** (9.21 μM), is very similar to the one measured for compound **1**, indicating
103 that the structural modification has no impact on its biological activity.

104   To conclude, this study enabled the rapid identification of one new compound from *M. scaber*.
105 The biological activity evaluation highlighted the ability of compounds **1** and **2** to inhibit the
106 production of Il-8, confirming the importance of *M. scaber* metabolites and their possible uses in
107 cosmetics and personal care products.

3. Materials and Methods

General procedure

110   The preparative HPLC was performed on a VWR LaPrep P110 system using a C-630 Büchi
111 UV detector. NMR spectra acquisition was realized using a 600 MHz Bruker Avance spectrometer
112 equipped with Z-gradients and a triple resonance TXI probe. The signals were referenced in ppm to
113 the residual solvent signals (CD$_3$OD, at δ_H 3.31 and δ_C 49.0). The infra-red spectrum was acquired
114 on a Nicolet IS50 FT-IR spectrophotometer. The specific rotation was measured using a Anton Paar
115 MCP150 polarimeter.

Plant material

117   The flowered aerial parts of *Mitracarpus Scaber* were collected in Burkina Faso in the town of
118 Poun and then dried in the same area.

Extraction and purification

120   An ethanolic extraction was performed on a 300 g sample of dried plant with a ratio
121 plant/solvent of 1/7 yealding 16.5 g of crude extract which was then directly processed by reverse
122 phase with an XBridge Prep C18, 5 μm (OBD 30 × 250 mm) preparative HPLC column. A gradient
123 H$_2$O/MeOH (starting from 90:10 to 70/30 in 30 minutes at 100 mL min^{-1}) was used to afford the
124 compounds **1** (84 mg) and **2** (113 mg).

LC-MS data acquisition and processing

126   A XEVO-G2 XS QTOF (Waters) equipped with an electrospray ionization (ESI) source was used
127 for the qualitative analysis of the extract. A first screening analysis was performed using the MS^E
128 technology (Waters) on a mass range from 50 to 1500 Da. The optimal ionization source working
129 parameters were as follows: capillary voltage, 3.0 kV; sampling cone, 40 V; extraction cone, 6.0 V;
130 source temperature, 150 °C; desolvation temperature, 600 °C; cone gas flow, 50 L/h; desolvation gas
131 flow, 1000 L/h. MS/MS data were obtained using a data-dependent analysis (DDA) with the same
132 ionization parameters as above using three different collision energies: 10, 20 and 40 V.

Construction of the molecular network

134   A molecular network was created using the online workflow at GNPS[3]. The data were filtered
135 by removing all MS/MS peaks within +/- 17 Da of the precursor m/z. MS/MS spectra were window
136 filtered by choosing only the top 6 peaks in the +/- 50 Da window throughout the spectrum. The data
137 were then clustered with MS-Cluster with a parent mass tolerance of 2.0 Da and a MS/MS fragment
138 ion tolerance of 0.5 Da to create consensus spectra. Furthermore, consensus spectra that contained
139 less than 2 spectra were discarded. A network was then created where edges were filtered to have a
140 cosine score above 0.7 and more than 3 matched peaks. Furthermore, edges between two nodes were
141 kept in the network if and only if each of the nodes appeared in each other's respective top 10 most
142 similar nodes. The spectra in the network were then searched against GNPS' spectral libraries. The

library spectra were filtered in the same manner as the input data. All matches kept between network spectra and library spectra were required to have a score above 0.7 and at least 6 matched peaks.

Energy resolved mass spectrometry

The LTQ-Orbitrap XL mass spectrometer (Thermo Scientific (Bremen), Bremen, Germany) was used for the ERMS study. The analysis was performed in positive ion mode with a mass range of m/z 100–1100. The optimized ESI parameters were set as follows: capillary temperature of 250 °C; sheath gas (nitrogen) flow of 30 arb.; auxiliary gas (nitrogen) flow of 10 arb.; source voltage of 4.25 kV; capillary voltage of 25 V; tube lens voltage of 110 V. The resolution of the orbitrap mass analyzer was set at 30,000. The isolation width was 2 amu, and the normalized collision energy (CE) was set from 10 to 20. Collision-induced dissociation (CID) was conducted in LTQ with an activation q of 0.25 and activation time of 30 ms. All instruments were controlled by the Xcalibur data system, and the data acquisition was carried out by analyst software Xcalibur (version 2.1) (Waltham, MA, USA) from Thermo Electron Corp.

Synchrotron Radiation Circular Dichroism

The SRCD experiments were carried out on the SRCD station [20] DISCO beamline [21] at the SOLEIL synchrotron (Gif-sur-Yvette, France). The samples were placed in calcium fluoride cells of 100 microns optical path length and measured at 0.2 mol/l in methanol. (+)-camphor-10-sulfonic acid (CSA) solution was used to calibrate the SRCD signal. For each sample, three spectra were collected in the 350–200 nm range with 1 nm step and 1200 ms integration time. The molar circular dichroism $\Delta\epsilon$ is expressed in M^{-1} cm^{-1}.

Computational details

All QM calculations were carried out using Gaussian 16[22]. The energy scan of the C–O bonds was performed using the Hartree–Fock method at the STO-3G level and a 0.1 Å bond length step. The GMMX package was used for the conformational analysis (force field: MMFF94). The TD DFT calculations were performed using the B3LYP method at the 6-31G(d) level for 20 excited states. The SpecDis 1.71 software was used to plot the ECD spectrum[23].

Cell culture

HaCaT Keratinocytes cells were cultured under standard conditions in DMEM medium supplemented with 10% fetal calf serum. The medium was changed every second day. Confluent cultures were removed by trypsin incubation, and then the cells were counted. They were seeded into 96-well culture microplates at a density of 30,000 cells per well (200 μ L) and kept at 37 °C for 24 h.

Interleukine release measurement

The release of IL-8 in cell supernatants was determined by ELISA. After TNF-α incubation (0.5 ng/mL), cell supernatants were harvested and stored at -20 °C until use for measurements. The quantity of released Il-8 was measured according to the manufacturer's instructions (Kit ELISA Human CXCL8 / IL8 R&D Systems). The decrease in Il-8 production by EGCG (10 μg/mL) validated the method.

Statistical analyses

All statistical analyses were performed using R 3.5.0 [24]. Cell samples were analyzed by repeated-measures (n=4) one-way analysis of variance (ANOVA) followed by a Tukey's range test. Significant differences for both clarinoside (**1**) and harounoside (**2**) were relative to control as indicated. NS. not significant; *$P < 0.05$; ***$P < 0.001$

Compound Characterization

1: White, amorphous solid; $[\alpha]_D^{20}$ +12.8 (c 0.1, CH_3OH); UV (DAD) λ_{max} 223, 245, 284, 346 nm; ^1H NMR and ^{13}C NMR data see Table 1; HRESIMS (+) m/z 545.1685 [M + Na]$^+$ (545,16295 calcd. for $C_{25}H_{30}O12Na$, Δ -1.8 ppm).

Bibliography

1. Olivon, F.; Allard, P.M.; Koval, A.; Righi, D.; Genta-Jouve, G.; Neyts, J.; Apel, C.; Pannecouque, C.; Nothias, L.F.; Cachet, X.; Marcourt, L.; Roussi, F.; Katanaev, V.L.; Touboul, D.; Wolfender, J.L.; Litaudon, M. Bioactive Natural Products Prioritization Using Massive Multi-informational Molecular Networks. *ACS Chemical Biology* **2017**, *12*, 2644–2651. PMID: 28829118.

2. Nothias, L.F.; Nothias-Esposito, M.; da Silva, R.; Wang, M.; Protsyuk, I.; Zhang, Z.; Sarvepalli, A.; Leyssen, P.; Touboul, D.; Costa, J.; Paolini, J.; Alexandrov, T.; Litaudon, M.; Dorrestein, P.C. Bioactivity-Based Molecular Networking for the Discovery of Drug Leads in Natural Product Bioassay-Guided Fractionation. *Journal of Natural Products* **0**, *0*, null.

3. Wang, M.; Carver, J.J.; Phelan, V.V.; Sanchez, L.M.; Garg, N.; Peng, Y.; Nguyen, D.D.; Watrous, J.; Kapono, C.A.; Luzzatto-Knaan, T.; Porto, C.; Bouslimani, A.; Melnik, A.V.; Meehan, M.J.; Liu, W.T.; Crüsemann, M.; Boudreau, P.D.; Esquenazi, E.; Sandoval-Calderón, M.; Kersten, R.D.; Pace, L.A.; Quinn, R.A.; Duncan, K.R.; Hsu, C.C.; Floros, D.J.; Gavilan, R.G.; Kleigrewe, K.; Northen, T.; Dutton, R.J.; Parrot, D.; Carlson, E.E.; Aigle, B.; Michelsen, C.F.; Jelsbak, L.; Sohlenkamp, C.; Pevzner, P.; Edlund, A.; McLean, J.; Piel, J.; Murphy, B.T.; Gerwick, L.; Liaw, C.C.; Yang, Y.L.; Humpf, H.U.; Maansson, M.; Keyzers, R.A.; Sims, A.C.; Johnson, A.R.; Sidebottom, A.M.; Sedio, B.E.; Klitgaard, A.; Larson, C.B.; Boya P, C.A.; Torres-Mendoza, D.; Gonzalez, D.J.; Silva, D.B.; Marques, L.M.; Demarque, D.P.; Pociute, E.; O'Neill, E.C.; Briand, E.; Helfrich, E.J.N.; Granatosky, E.A.; Glukhov, E.; Ryffel, F.; Houson, H.; Mohimani, H.; Kharbush, J.J.; Zeng, Y.; Vorholt, J.A.; Kurita, K.L.; Charusanti, P.; McPhail, K.L.; Nielsen, K.F.; Vuong, L.; Elfeki, M.; Traxler, M.F.; Engene, N.; Koyama, N.; Vining, O.B.; Baric, R.; Silva, R.R.; Mascuch, S.J.; Tomasi, S.; Jenkins, S.; Macherla, V.; Hoffman, T.; Agarwal, V.; Williams, P.G.; Dai, J.; Neupane, R.; Gurr, J.; Rodríguez, A.M.C.; Lamsa, A.; Zhang, C.; Dorrestein, K.; Duggan, B.M.; Almaliti, J.; Allard, P.M.; Phapale, P.; Nothias, L.F.; Alexandrov, T.; Litaudon, M.; Wolfender, J.L.; Kyle, J.E.; Metz, T.O.; Peryea, T.; Nguyen, D.T.; VanLeer, D.; Shinn, P.; Jadhav, A.; Müller, R.; Waters, K.M.; Shi, W.; Liu, X.; Zhang, L.; Knight, R.; Jensen, P.R.; Palsson, B.Ø.; Pogliano, K.; Linington, R.G.; Gutiérrez, M.; Lopes, N.P.; Gerwick, W.H.; Moore, B.S.; Dorrestein, P.C.; Bandeira, N. Sharing and community curation of mass spectrometry data with Global Natural Products Social Molecular Networking. *Nature Biotechnology* **2016**, *34*, 828 EP –.

4. Ekpendu, T.O.; Akah, P.A.; Adesomoju, A.A.; Okogun, J.I. Antiinflammatory and Antimicrobial Activities of *Mitracarpus scaber* Extracts. *International Journal of Pharmacognosy* **1994**, *32*, 191–196.

5. Bisignano, G.; Sanogo, R.; Marino, A.; Aquino, R.; 'angelo, V.D.; Germano, M.P.; De Pasquale, R.; Pizza, C. Antimicrobial activity of *Mitracarpus scaber* extract and isolated constituents. *Letters in Applied Microbiology* **2000**, *30*, 105–108.

6. Gbaguidi, F.; Accrombessi, G.; Moudachirou, M.; Quetin-Leclercq, J. HPLC quantification of two isomeric triterpenic acids isolated from Mitracarpus scaber and antimicrobial activity on Dermatophilus congolensis. *Journal of Pharmaceutical and Biomedical Analysis* **2005**, *39*, 990 – 995.

7. Okunade, A.L.; Clark, A.M.; Hufford, C.D.; Oguntimein, B.O. Azaanthraquinone: An Antimicrobial Alkaloid from *Mitracarpus scaber*. *Planta Medica* **1999**, *65*, 447–448.

8. Harouna, H.; Faure, R.; Elias, R.; Debrauwer, L.; Saadou, M.; Balansard, G.; Boudon, G. Harounoside a pentalongin hydroquinone diglycoside from Mitracarpus scaber. *Phytochemistry* **1995**, *39*, 1483 – 1484.

9. Pialat, J.P.; Hoffmann, P.; Moulis, C.; Fouraste, I.; Labidalle, S. Synthesis and Extraction of Pentalongin, A Naphthoquinoid From Mitracarpus Scaber. *Natural Product Letters* **1998**, *12*, 23–30.

10. Burgess, K.; Borutzki, Y.; Rankin, N.; Daly, R.; Jourdan, F. MetaNetter 2: A Cytoscape plugin for ab initio network analysis and metabolite feature classification. *Journal of Chromatography B* **2017**.

11. Menachery, S.P.M.; Laprévote, O.; Nguyen, T.P.; Aravind, U.K.; Gopinathan, P.; Aravindakumar, C.T. Identification of position isomers by energy-resolved mass spectrometry. *Journal of Mass Spectrometry* **2015**, *50*, 944–950.

12. Xia, B.; Zhou, Y.; Liu, X.; Xiao, J.; Liu, Q.; Gu, Y.; Ding, L. Use of electrospray ionization ion-trap tandem mass spectrometry and principal component analysis to directly distinguish monosaccharides. *Rapid Communications in Mass Spectrometry* **2012**, *26*, 1259–1264.

13. Giner, J.L.; Feng, J.; Kiemle, D.J. NMR Tube Degradation Method for Sugar Analysis of Glycosides. *Journal of Natural Products* **2016**, *79*, 2413–2417. PMID: 27603739.

14. Genta-Jouve, G.; Weinberg, L.; Cocandeau, V.; Maestro, Y.; Thomas, O.P.; Holderith, S. Revising the Absolute Configurations of Coatlines via Density Functional Theory Calculations of Electronic Circular Dichroism Spectra. *Chirality* **2013**, *25*, 180–184.

15. Han, A.R.; Park, S.R.; Park, J.W.; Lee, E.Y.; Kim, D.M.; Kim, B.G.; Yoon, Y.J. Biosynthesis of Glycosylated Derivatives of Tylosin in Streptomyces venezuelae. *J. Microbiol. Biotechnol* **2011**, *21*, 613–616.

16. De Castro, C.; Kenyon, J.J.; Cunneen, M.M.; Molinaro, A.; Holst, O.; Skurnik, M.; Reeves, P.R. The O-specific polysaccharide structure and gene cluster of serotype O:12 of the *Yersinia pseudotuberculosis* complex, and the identification of a novel l-quinovose biosynthesis gene. *Glycobiology* **2013**, *23*, 346–353.

17. Baggiolini, M.; Clark-Lewis, I. Interleukin-8, a chemotactic and inflammatory cytokine. *FEBS Letters* **1992**, *307*, 97–101.

18. Pease, J.E.; Sabroe, I. The Role of Interleukin-8 and its Receptors in Inflammatory Lung Disease. *American Journal of Respiratory Medicine* **2002**, *1*, 19–25.

19. of EGCG has been measured on a previous experiment., T.I.

20. Réfrégiers, M.; Wien, F.; Ta, H.P.; Premvardhan, L.; Bac, S.; Jamme, F.; Rouam, V.; Lagarde, B.; Polack, F.; Giorgetta, J.L.; Ricaud, J.P.; Bordessoule, M.; Giuliani, A. DISCO synchrotron-radiation circular-dichroism endstation at SOLEIL. *Journal of Synchrotron Radiation* **2012**, *19*, 831–835.

21. Giuliani, A.; Jamme, F.; Rouam, V.; Wien, F.; Giorgetta, J.L.; Lagarde, B.; Chubar, O.; Bac, S.; Yao, I.; Rey, S.; Herbeaux, C.; Marlats, J.L.; Zerbib, D.; Polack, F.; Réfrégiers, M. DISCO: A low-energy multipurpose beamline at synchrotron SOLEIL. *Journal of Synchrotron Radiation* **2009**, *16*, 835–841.

22. Frisch, M.J.; Trucks, G.W.; Schlegel, H.B.; Scuseria, G.E.; Robb, M.A.; Cheeseman, J.R.; Scalmani, G.; Barone, V.; Petersson, G.A.; Nakatsuji, H.; Li, X.; Caricato, M.; Marenich, A.V.; Bloino, J.; Janesko, B.G.; Gomperts, R.; Mennucci, B.; Hratchian, H.P.; Ortiz, J.V.; Izmaylov, A.F.; Sonnenberg, J.L.; Williams-Young, D.; Ding, F.; Lipparini, F.; Egidi, F.; Goings, J.; Peng, B.; Petrone, A.; Henderson, T.; Ranasinghe, D.; Zakrzewski, V.G.; Gao, J.; Rega, N.; Zheng, G.; Liang, W.; Hada, M.; Ehara, M.; Toyota, K.; Fukuda, R.; Hasegawa, J.; Ishida, M.; Nakajima, T.; Honda, Y.; Kitao, O.; Nakai, H.; Vreven, T.; Throssell, K.; Montgomery, Jr., J.A.; Peralta, J.E.; Ogliaro, F.; Bearpark, M.J.; Heyd, J.J.; Brothers, E.N.; Kudin, K.N.; Staroverov, V.N.; Keith, T.A.; Kobayashi, R.; Normand, J.; Raghavachari, K.; Rendell, A.P.; Burant, J.C.; Iyengar, S.S.; Tomasi, J.; Cossi, M.; Millam, J.M.; Klene, M.; Adamo, C.; Cammi, R.; Ochterski, J.W.; Martin, R.L.; Morokuma, K.; Farkas, O.; Foresman, J.B.; Fox, D.J. Gaussian~16 Revision B.01, 2016. Gaussian Inc. Wallingford CT.

23. Bruhn, T.; Schaumlöffel, A.; Hemberger, Y.; Bringmann, G. SpecDis: Quantifying the Comparison of Calculated and Experimental Electronic Circular Dichroism Spectra. *Chirality* **2013**, *25*, 243–249.

24. R Core Team. *R: A Language and Environment for Statistical Computing*. R Foundation for Statistical Computing, Vienna, Austria, 2018.

Sample Availability: Samples of the compounds **1** and **2** are available from the authors.